DOI: 10.1002/cbic.200800716

Bacterial Glycoprofiling by Using Random Sequence Peptide Microarrays

Carlos Morales Betanzos,[a] Maria J. Gonzalez-Moa,[a] Kathryn W. Boltz,[a] Brian D. Vander Werf,[a] Stephen Albert Johnston,[a, b] and Sergei A. Svarovsky*[a]

Current analytical methods have been slow in addressing the growing need for glyco-analysis. A new generation of more empirical high-throughput (HTP) tools is needed to aid the advance of this important field. To this end, we have developed a new HTP screening platform for identification of surface-immobilized peptides that specifically bind O-antigenic glycans of bacterial lipopolysaccharides (LPS). This method involves screening of random sequence peptide libraries in addressable high-density microarray format with the newly developed luminescent LPS–quantum dot micelles. Screening of LPS fractions from O111:B4 and O55:B5 serotypes of *E. coli* on a microarray consisting of 10 000 20-mer peptide features revealed minor differences, while comparison of LPS from *E. coli* O111:B4 and *P. aeruginosa* produced sets of highly specific peptides. Peptides strongly binding to the *E. coli* LPS were highly enriched in aromatic and cationic amino acids, and most of these inhibited growth of *E. coli*. Flow cytometry and isothermal titration calorimetry (ITC) experiments showed that some of these peptides bind LPS in-solution with a K_d of 1.75 μM. Peptide selections against *P. aeruginosa* were largely composed of hydrogen-bond forming amino acids in accordance with dramatic compositional differences in O-antigenic glycans in *E. coli* and *P. aeruginosa*. While the main value of this approach lies in the ability to rapidly differentiate bacterial and possibly other complex glycans, the peptides discovered here can potentially be used off-array as antiendotoxic and antimicrobial lead compounds, and on-array/on-bead as diagnostic and affinity reagents.

Introduction

The increasing awareness of the importance of glycosylation to biological systems has led to recognition of the need to develop better tools for the analysis of protein–carbohydrate interactions. In contrast to template-driven nucleic acid and protein sequences, which aid function assignments, the need for a more empirical, high-throughput analysis of potential carbohydrate patterns has resulted in a variety of approaches.[1] The two key newcomers in the area of functional glycomics thus far have been glycan[2] and lectin microarrays,[3] in which glycans or lectins are immobilized on glass slides for investigating the specificity of glycan-binding proteins or glycoconjugates, respectively. In lectin microarrays, carbohydrate-binding proteins, such as lectins and anticarbohydrate antibodies, are immobilized on a solid support in high spatial density. Interrogation of these arrays with fluorescently-labeled samples creates binding patterns (glycosignatures) that depend on the carbohydrate structures present, and provide a method for rapid characterization of glycans on glycoproteins,[4] bacteria,[5] or mammalian cells.[6] The microarray format allows rapid parallel analysis of multiple carbohydrate–protein interactions with a minimal amount of sample. Notwithstanding the advantages, lectin microarrays are intrinsically handicapped by restricted availability,[3] and the limited and often unexpected specificities of natural lectins.[7] Only about 60 lectins are commercially available, and they have the ability to recognize only a fraction of glycans present on mammalian and especially on microbial cells.[3] The common problems inherent to other protein arrays,[8] such as linking chemistry, orientation-dependent binding activity, and storability, are also important factors that strongly argue in favor of alternative approaches.

Proteins are not the only molecules that bind carbohydrates. Cyclic tricatechol[9] and terphenyl[10] constructs, acyclic pyridine, pyrimidine, and naphthyridine units,[11] self-assembled structures and various boronic acid derivatives[12,13] have been described. Also, aptamers and peptides have been explored.[14] Synthetic peptides have long been known as highly versatile molecules for a variety of biological applications. Unlike proteins, which unfold readily and subsequently lose their biological activities, peptides are functionally stable and capable of retaining their activities under most reaction conditions; this makes them the preferred molecules for facile and robust screening assays, especially in microarray-based formats.

We have an ongoing program applying addressable random sequence peptide microarrays, as an alternative to phage dis-

[a] *C. Morales Betanzos,[+] Dr. M. J. Gonzalez-Moa,[+] Dr. K. W. Boltz, B. D. Vander Werf, Dr. S. A. Johnston, Dr. S. A. Svarovsky*
Center for Innovations in Medicine, The Biodesign Institute
Arizona State University, 1001 S. McAllister Avenue
Tempe, AZ 85287 (USA)
Fax: (+1) 480-727-0756
E-mail: sergei.svarovsky@asu.edu

[b] *Dr. S. A. Johnston*
School of Life Sciences, Arizona State University
1711 South Rural Road, Tempe, AZ 85287 (USA)

[+] *These authors contributed equally to this work.*

Supporting information for this article is available on the WWW under http://dx.doi.org/10.1002/cbic.200800716

play, to the analysis of various biomolecular interactions. As a part of this program, we have tested these microarrays for their ability to detect carbohydrate interactions. We hypothesized that owing to the large chemical diversity of peptide structures with no preconceived specificity, the microarray could provide an expedient approach to de novo discovery of artificial lectin mimics with engineered specificities towards glycans of interest. As a proof-of-concept, we chose to use the microarray to analyze the saccharidic portion of bacterial lipopolysaccharides (LPS). The reason for choosing such a complex target was threefold. First, the diversity of glycan structures unique to bacteria would allow the widest dynamic range of molecules to be tested and therefore let us evaluate the limitations of this approach. Second, from a practical standpoint LPS have been implicated in the systemic inflammatory response and septic shock, which have claimed more than 200 000 lives each year in the U.S. alone.[15] Hence, there is a great deal of interest in developing therapeutic agents that can efficiently bind LPS.[16] Third, whereas the therapeutic strategy directed against viral glycans was a success, a similar approach to antibacterial therapies has not been systematically explored due to difficulties in finding molecules that can selectively bind to bacterial glycans.[17]

Herein, we report our findings in screening of 10 000 random 20-mer peptide sequences printed on a glass slide with newly developed luminescent LPS glycoprobes for potential lectinomimetic activity. A set of specific lectinomimetic antagonists of LPS molecules have been discovered that can be used as a new class of diagnostic, antiendotoxic, and antimicrobial peptide leads in both on- and off-array formats. To our knowledge, this is the first application of peptide microarrays to studying carbohydrate interactions.

Results and Discussion

General experimental set-up

The peptide microarrays were constructed by spotting 10 000 random 20-mer sequences in duplicates on a maleimide-functionalized microscope glass slide by using a robotic pin spotter. The random peptide library was produced by conventional solid-phase synthesis based on computer-generated random sequences of 19 amino acids, excluding cysteine, for the first 17 amino acids. A C-terminal –GSC sequence was incorporated into each peptide to facilitate coupling to the array surface. These arrays were probed directly with fluorescently labeled LPS.

General considerations in the design of LPS glycoprobes

LPS is a complex, negatively charged lipoglycan composed of three distinct regions: 1) a fatty acid region called lipid A that has very low variability; 2) a conserved glycosidic "core" consisting of approximately ten monosaccharides; and 3) a highly variable region called O-antigen, consisting of repetitive subunits of one to eight monosaccharides repeated up to 100 times.[18] The O-antigen region defines the strain, serotype, and even the virulence of the bacteria; this makes it a very attractive target to study. Probing the peptide microarray with directly labeled LPS allowed us to avoid the use of secondary detection reagents, which complicate the interpretation and later deconvolution of the data. This consideration is especially important for the random peptide microarrays because each peptide on the array de facto is not specific and serves as a putative ligand for any target of choice. Not only can the secondary probe bind to the array, but it could also compete with the primary probe. In the case of carbohydrates, the binding affinities of which are typically weak, the latter can present a serious problem. For these reasons, the arrays were probed directly with conventional organic dye-labeled and the newly developed quantum dot (Qdot)-labeled LPS in order to specifically single out carbohydrate interactions.

LPS labeling with Qdots

The existing LPS labeling strategies rely on chemical modification of LPS molecules with organic dyes (Figure 1 A). This method requires complex manipulation and purification steps, is not site-specific, and depends on the availability of reactive groups in the LPS molecule.[19] When such groups are unavailable, an extra functionality is introduced into the saccharidic branch of LPS, which might affect its physical properties and biomolecular recognition events; thus it is not ideally suitable for the purposes of this study. For this reason, we have developed an alternative labeling strategy that takes advantage of the amphipathic nature of LPS molecule and does not introduce any new chemical modalities into the structure.

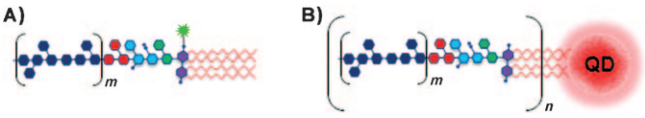

Figure 1. A cartoon depicting: A) organic dye labeled LPS; B) Qdots-labeled LPS; *m* designates the number of O-antigen repeating units, *n* designates the number of LPS molecules attached to the Qdot.

We used nanometer-sized crystals of semiconductors known as quantum dots (Qdots) that have recently emerged as useful luminescent labeling agents.[20] Coating of hydrophobic Qdots with phospholipids[21] and synthetic amphiphilic polymers have been previously described.[22] Both methods rely on phase transfer of hydrophobic Qdots from organic solvent to an aqueous solution of an amphiphile. Using a similar approach, we conjugated smooth-type LPS from *E. coli* and *P. aeruginosa* to hydrophobic Qdots (Figure 1 B). In this case, the lipid A, which is responsible for self-aggregation, also confers the ability of LPS to bind to hydrophobic surfaces of Qdots. Since the lipid functionality is attached directly to the label, Qdot–LPS constructs are especially useful for studying the saccharidic moiety of LPS.

Comparison of Qdot- and organic dye-labeled LPS

Although many peptides have been shown to bind LPS in solution,[23] at the outset of this work it was not clear if peptides in the microarray format would also be able to bind LPS specifically and reproducibly. In order to demonstrate that the peptides on the microarray indeed bind LPS and the interaction is not dye- or lipid-induced, we conducted several experiments. In the first of these experiments, identical concentrations of LPS from *E. coli* O111:B4 (EC_{O111}) labeled with FITC (FITC–EC_{O111}) and with Qdots (QDot–EC_{O111}) were used to probe the microarray slides. The "unblocked" sample was used as is, while the "blocked" sample was spiked with 100-fold excess of unlabeled EC_{O111} during the binding step. For both FITC–EC_{O111} and QDot–EC_{O111} probes (Figure S1 in the Supporting Information) blocking with unlabeled LPS localized the specific interactions, as most of the top binders to LPS become low binders when excess unlabeled LPS is used to inhibit the specific peptide–LPS interactions. This simple test effectively eliminated any unspecific dye-induced interactions. The same test was applied to all binding experiments described below.

To test the applicability of the Qdot–LPS probes for specifically detecting carbohydrate-binding events, we used scatter plots as previously reported by Reddy and Kodadek,[24] and compared the results with those obtained with conventionally labeled LPS. This representation helped us to focus our attention only on peptides with high expression profile for both experiments (FITC–EC_{O111} and Qdot–EC_{O111}). Figure 2 shows reasonable correlation ($R = 0.824$) between the two experiments. Although some unique hits were present both in Qdot–LPS and FITC–LPS binding peptides, they can be attributed to differences in the probe construction and photophysical properties of the labels. The LPS is presented on the multivalent Qdots in a defined orientation, since the hydrophobic Qdots only exist in aqueous solution when they are enclosed in the hydrophilic environment created by the lipid portion of the LPS molecules. This orientation exposes the saccharidic branch of the LPS, similar to their orientation in the micellar (or cellular) state of LPS. In contrast the monovalent FITC–LPS probe can potentially detect saccharidic-, dye-, and lipid-induced interactions. It has been found that aggregated micellar FITC–LPS has strongly diminished fluorescence due to quenching, while the disaggregation of single FITC–LPS molecules from micelles leads to enhancement in fluorescence.[25] So, it is likely that oriented micellar LPS molecules would not be observable, and the most significant signal detected would come from the single LPS molecules, which include nonsaccharidic components. Due to the well-known cluster glycoside effect,[26] the in-

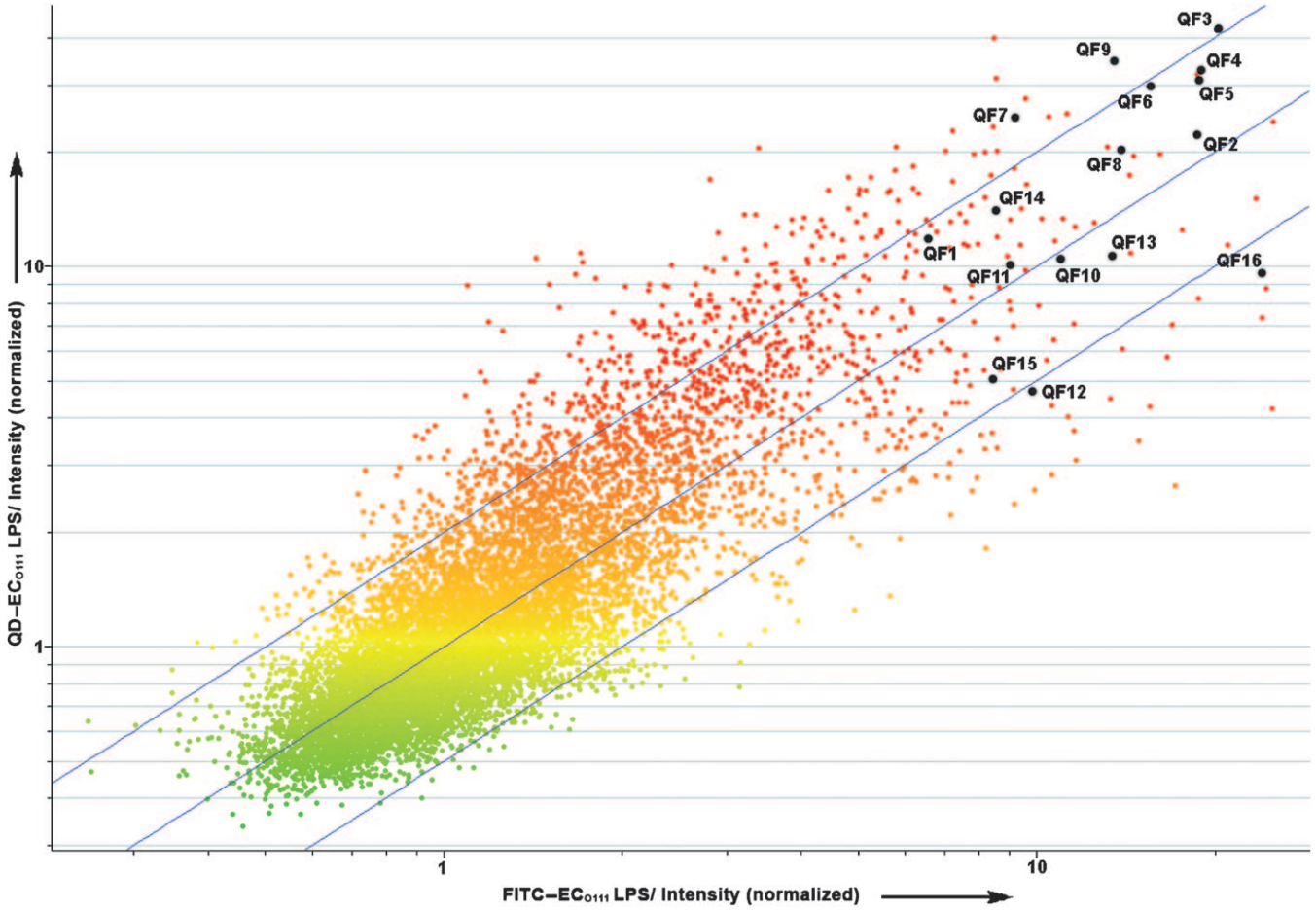

Figure 2. FITC-labeled versus Qdot-labeled *E. coli* O111:B4 LPS correlation ($R = 0.824$). Annotated black dots indicate selected LPS-binding peptides shown in Table 1. Both axes show normalized signal in a logarithmic (log2) scale. Blue lines delimit the twofold change.

teraction of multiple sugars is also stronger than a single LPS molecule. These observations highlight the utility of Qdot–LPS for studying variable saccharidic components.

Selection of peptides binding the saccharidic branch of LPS

Since the Qdot labels were novel for LPS, we argued that only peptides that bind both FITC–LPS and Qdot–LPS with high intensity were the most reliable saccharidic LPS-binding peptides. Such peptides were identified by statistical analysis by using image-processed data, and visualized as a scatter plot.[24] We have selected only high intensity binders with a minimal standard deviation ($\sigma < 0.2$) that were present in both Qdot–LPS and FITC–LPS experiments (Figure 2). Autofluorescent peptides were filtered as described in the Experimental Section and each hit was independently confirmed by careful visual inspection of the slides.

The data revealed 16 peptides, QF1–QF16, that bound with high affinity to *E. coli* O111:B4 LPS (Table 1). Most of these peptides contain noticeably abundant cationic arginine, lysine, and histidine, along with clusters of aromatic hydrophobic tryptophan and phenylalanine and/or tyrosine. Since many of the existing LPS-binding peptides are also antimicrobial,[27] we hypothesized that if our selections were valid then at least some of the peptides should share sequence similarity with the existing antimicrobial peptides (AMPs). To test this hypothesis, we compared the selected sequences against several AMP databases. In particular, we found that the above amino acids were also abundant in indolicidin-like AMPs.[28] Moreover, using the Antimicrobial Peptide Database,[29] we found that some of these peptides (QF1–8) shared 30 to 40% similarity to human histatins-2, -6, or -9, which are histidine-rich AMPs found in oral cavities. Finally, we applied a recently developed algorithm that predicts antibacterial sequences based on similarity to the existing 486 AMPs.[30] The higher the antibacterial peptides prediction (APP) score, the more probable the antibacterial activity, while negative scores suggest no antibacterial activity. The APP scores shown in Table 1 predicted that 11 out of 16 selected peptides had potential antibacterial properties.

Antimicrobial properties of the LPS binding peptides

We assayed the ability of the LPS-binding peptides to inhibit *E. coli* growth, and compared them to 142 LPS nonbinding peptides (Table S1). Figure 3 shows that nearly 70% of the LPS-binding peptides demonstrated some growth inhibition activity against *E. coli* DH10B, while none of the 142 nonbinding peptides inhibited growth by more than 20% (Figure S2). Interestingly, the peptides QF12, -13, -14, and -16 demonstrated enhancement of bacterial growth (Figure 3). In agreement with the APP scores peptides QF1–10 displayed antibacterial activity (Table 1). An evident outlier, QF15, which departs from the conventional cationic amphipathic motifs associated with AMPs, was also identified. Further testing through kinetic growth curves showed that these peptides are bacteriostatic, not bactericidal. This agrees with recent work demonstrating that the

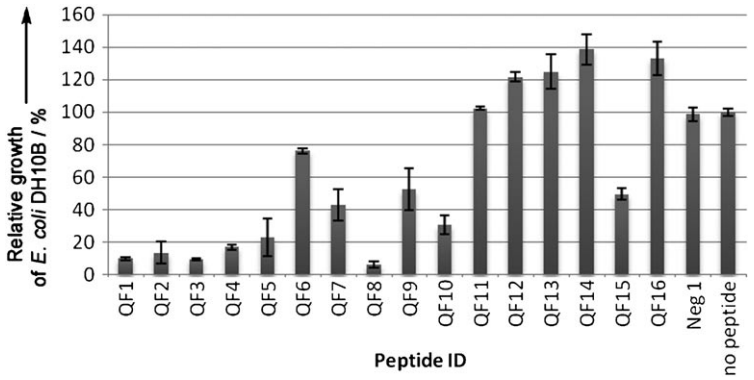

Figure 3. Relative growth inhibition activities of peptides QF1–16 tested against *E. coli* DH10B. The error bars are standard deviations of triplicate measurements; Neg1 is a negative control peptide.

Table 1. *E. coli* O111:B4 LPS binding peptides arranged by isoelectric point (pI), number of negative residues (NR), number of positive residues (PR), aliphatic index (AI), and antibacterial peptides prediction score (APP).[27]

ID	Peptide sequence	pI	NR	PR	AI	APP
QF1	RHWRKPRKWHKKWPPHRGSC	12.0	0	8	0	1.904
QF2	HRKHWRKRHKKHWKKRKGSC	12.0	0	11	0	2.673
QF3	HWKRRHKHKWPKRHPHKGSC	11.8	0	8	0	2.035
QF4	HFRKWHKRRWKHHKKWKGSC	11.8	0	9	0	2.155
QF5	WKKKRKHRHKKHWHPWRGSC	11.8	0	9	0	1.616
QF6	WKFRHRHHRHHWHKKWKGSC	11.8	0	7	0	2.167
QF7	WFWKHKKWRRHPRKWHWGSC	11.8	0	7	0	1.567
QF8	HRKPKFRHHHFKWKHWKGSC	11.2	0	7	0	1.529
QF9	WWHHKWFKHKKFWRHKFGSC	10.6	0	6	0	2.121
QF10	RVFKRYKRWLHVSRYYFGSC	10.6	0	6	49	1.296
QF11	VLKHHRVKAFKFWHEYIGSC	9.6	1	4	73	0.724
QF12	TWTQQMHHFRFSHKLERGSC	9.5	1	3	20	−0.566
QF13	THRPHNWYLFKNILFSHGSC	9.3	0	2	59	−0.964
QF14	GTNERYNMRKYHWWYWYGSC	9.0	1	3	0	−0.348
QF15	FQTAKLFFGYHNHTESSGSC	6.9	1	1	25	−0.036
QF16	EWHHIWINNQHYNHASHGSC	6.6	1	0	44	−0.795

biophysical properties required to kill bacteria differ from those to bind LPS.[31] In addition to affinity for LPS, bactericidal activity requires the abilities to traverse the LPS layer and to disaggregate LPS micelles. Our concentration-dependent studies (data not shown) demonstrated that even at 10 μM concentration, peptides QF7, -8, and -10 retained their ability to inhibit it up to 50% of *E. coli* growth.

Flow cytometry studies of the LPS-binding peptides

Intrigued by the high incidence of antimicrobial activity of the selected peptides, we conducted flow cytometry studies to quantify the in vivo binding abilities of the selected peptides to *E. coli*, and the ability of preincubation with LPS to block binding.[32] The LPS nonbinding peptide, Neg1, was used as a negative control. The peptides were biotinylated and their specificities were compared through quantifying the cell surface staining of *E. coli* DH10B cells with AlexaFluor488-labeled streptavidin. Cells labeled only with streptavidin were used as controls, and fluorescent intensity greater than that associated with streptavidin only labeled cells was quantified as the M1 region. Peptides QF1 through QF10 bound the cells almost completely in the M1 region; this indicates that these peptides bound the cells with higher affinity than would be expected from streptavidin-only binding (Table S2). The results for streptavidin, the negative control peptide Neg1, QF5, and QF8 are summarized in Figure 4. Both QF5 and QF8 bound to DH10B cells, and their cell-surface binding was nearly eliminated after preincubation with EC_{O111} LPS. While these results do not elucidate the nature of the target on the DH10B cell surface, they do show that the peptides bind to and are sequestered by the interaction with their target EC_{O111} LPS.

Surface plasmon resonance (SPR)

High resolution differential SPR was used to compare the binding of QF5, QF8, and Neg1 to EC_{O111} (Figures 5 and S3). This technique has sufficient sensitivity to detect direct binding of free glycans to lectins immobilized on a sensor chip and allows the evaluation of sugar–lectin dissociation constants in the nM range.[33] Both QF5 and QF8 are strong antimicrobial candidates, while Neg1—a peptide showing no binding to LPS on the peptide microarrays—was used as a negative control. The relative responses of these peptides were compared by using normalization based on the immobilization density and molecular weight of the respective peptides. Both QF5 and QF8 peptides had similar abilities to bind LPS, while Neg1 had negligible binding (Figure S3 A).

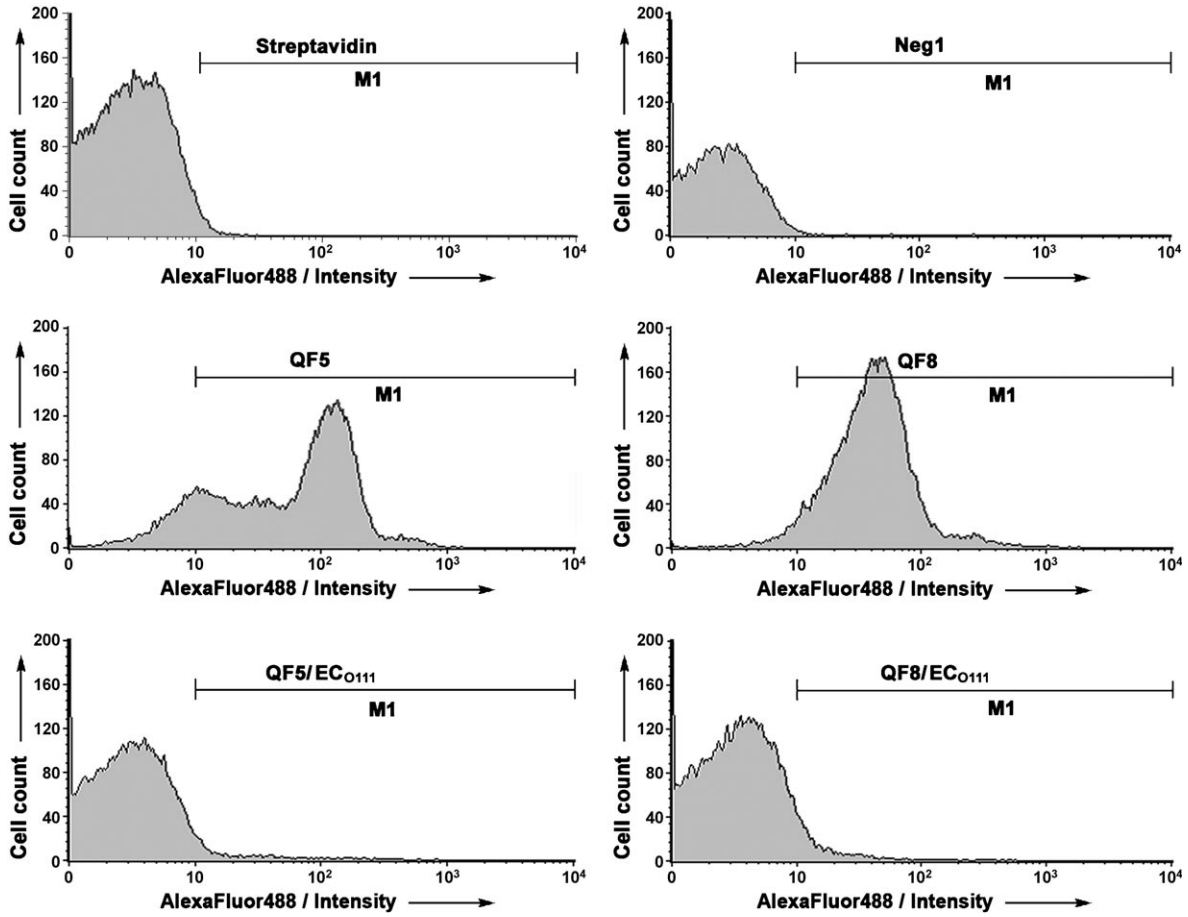

Figure 4. Flow cytometry of AlexaFluor488-labeled streptavidin, Neg1 control peptide, QF5, QF8, and QF5 and QF8 after 1 h preincubation with 100-fold excess of *E. coli* O111:B4 LPS. The *y* axes show the cell count, and the *x* axes show the AlexaFluor488 intensity.

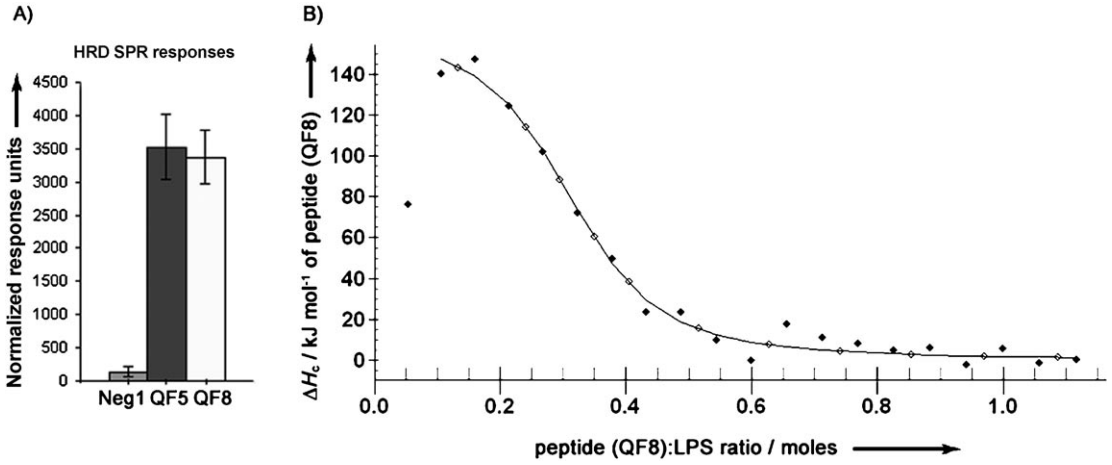

Figure 5. A) High resolution differential (HRD) SPR responses of peptides Neg1, QF5, and QF8 to *E. coli* O111:B4 LPS. B) ITC titration curve of the LPS EC_{O111} with peptide QF8.

Isothermal titration calorimetry (ITC)

To estimate the ability of peptide QF8, which exhibited maximal antimicrobial activity, to bind LPS in solution, we conducted the microcalorimetry titration of LPS EC_{O111} with QF8. The integrated heats in Figure 5B represent the net heats of each injection after subtraction of the heat of dilution of QF8 into pure buffer. The upward position of the ITC titration peaks (Figure S3B) and the resultant positive integrated heats indicate that the association between QF8 and LPS is an endothermic process.[34] With a single site independent binding model, the enthalpy (ΔH) of association between QF8 peptide and LPS is 7.8 kcal mol^{-1} with an equilibrium association constant (K_a) of 568 731 M^{-1} ($K_d = 1.75$ μM) and a stoichiometry of 0.2–0.4 QF8/LPS (due to heterogeneity of LPS) obtained at pH 7.4. This ratio likely corresponds to the net charge compensation between anionic LPS (2–4 negative charges) and cationic QF8 (seven positive charges).[35] The free energy (ΔG) and entropy (ΔS) changes of binding are estimated to be -7.8 kcal mol^{-1} and 52.6 cal mol^{-1} deg^{-1}, respectively.

Differentiation of *E. coli* serotypes

Gram-negative bacteria are classified by serological types (serotypes) based on the composition of the LPS O-antigen domains. Thus, the O-antigen, which is responsible for much of the immunospecificity of the bacterial cells, essentially serves as the "glycosignature" of a bacterium.[18] To test whether we can distinguish among different serotypes of a bacterium using the peptide microarray, we screened Qdot-labeled LPS derived from two different serotypes of *E. coli*: O111:B4 (EC_{O111}) and O55:B5 (EC_{O55}). Figure 6 shows the 2D scatter plot corresponding to these experiments. Overall, an excellent correlation ($R = 0.907$) was observed between the two serotypes; this indicates that there are only marginal differences detectable by the microarray. The high correlation coefficient is in agreement with the compositional similarity of the LPS molecules derived from the two serotypes (Figure 7). The O-antigen repeating units of EC_{O111}[36] and EC_{O55}[37] LPS are composed of five neutral monosaccharides, which include glucose (Glc), galactose (Gal), *N*-acetyl-galactosamine (GalNAc), *N*-acetylglucosamine (GlcNAc), and colitose (Col; 3,6-dideoxy-L-galactose). Although both structures differ in branching and sequence, the overall sugar content remains similar.

Despite the negligible statistical differences, a close visual inspection of the slides revealed several distinct hits that are unique to EC_{O111} (Figure 6, insert) and to EC_{O55}. In all the cases, for a hit to be statistically significant it must be reproduced in all replicate slides with a standard deviation of less than 0.2.

Differentiation between *E. coli* and *P. aeruginosa*

While the two *E. coli* serotypes have subtle compositional differences, more prominent differences are apparent when the LPS structures of *P. aeruginosa* 10 (PA_{10}) and EC_{O111} are compared (Figure 7). The repeating unit of PA_{10} consists of three unusual sugars: 2-*O*-acetyl-L-rhamnose (RhaAc), 2-*N*-acetyl-L-galacturonic acid (GalNA), and 2-*N*-acetyl-2,6-dideoxy-D-glucosamine (QuiN).[38] One of these sugars (GalNA) contains a carboxylic acid group that can carry negative charge and form strong hydrogen bonds. Screening of the PA_{10} LPS labeled with Qdots and statistical correlation of the results with EC_{O111} revealed a number of distinct hits for EC_{O111} and PA_{10}. Indeed, even a superficial visual inspection of the slides immediately shows differences in binding patterns between the two experiments (Figure 8).

Figure 9 shows the statistical correlation between Qdot–PA_{10} and Qdot–EC_{O111} experiments as a scatter plot.[24] The correlation coefficient is far lower ($R = 0.630$) than in the case of EC_{O111} versus EC_{O55} ($R = 0.907$; Figure 7). Peptides EC1–8 (Table 2), which specifically bind EC_{O111} but not PA_{10}, were identified by minimizing the error (standard deviation $\sigma < 0.2$) while maximizing the ratio of normalized EC_{O111} to PA_{10} signals. These comparisons independently validate the first selection of EC_{O111} binding peptides QF1–16 (Table 1) which are annotated in blue in Figure 9. A similar selection strategy seeking peptides that specifically bind PA_{10} but not EC_{O111} yielded peptides PA1–8

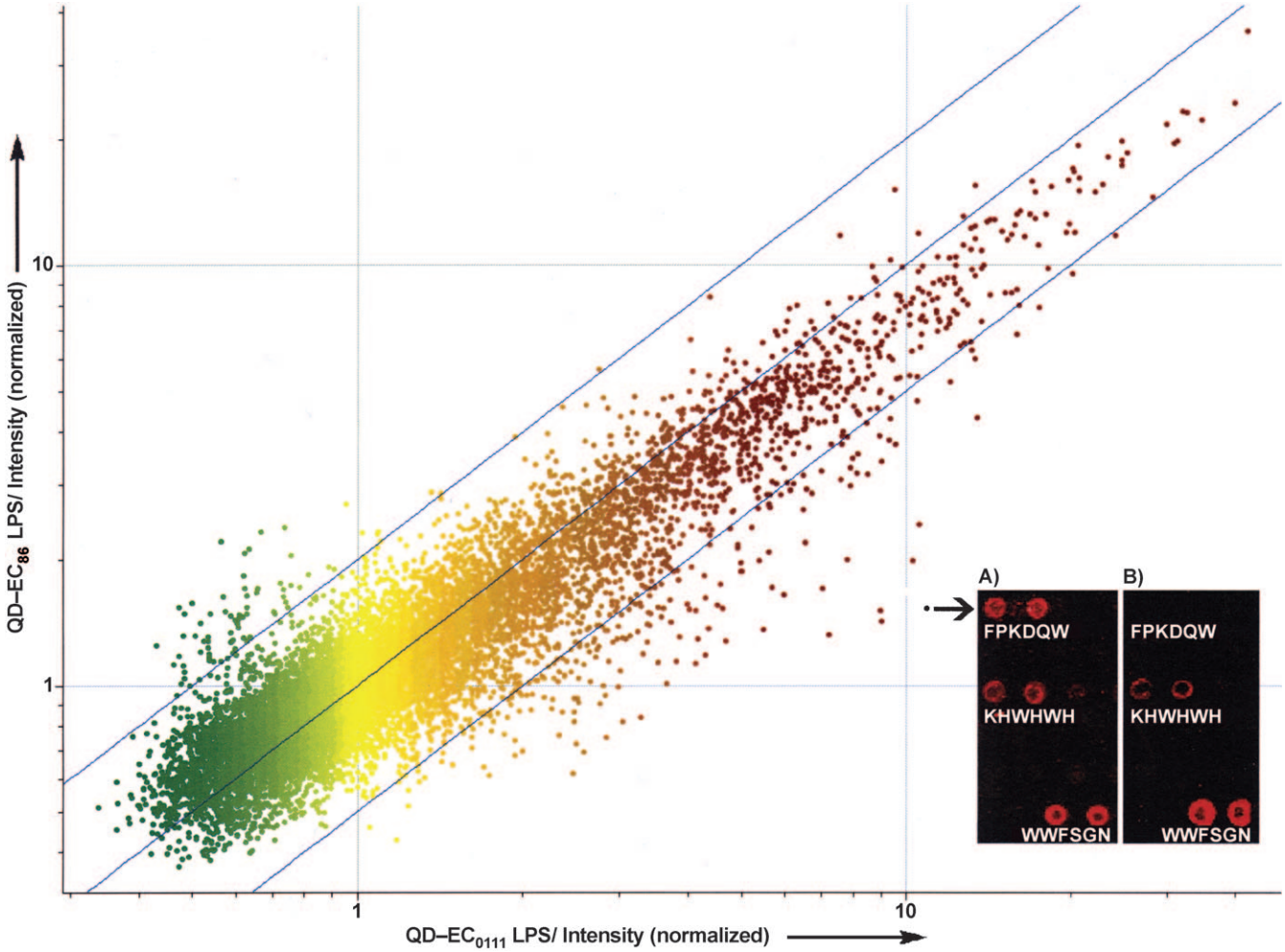

Figure 6. *E. coli* O111:B4 versus *E. coli* O55:B5 Qdot–LPS correlation for triplicate experiments of each ($R = 0.907$). The black dot corresponds to the EC_{O111} specific peptide FPKDQW (shown in the insert, with EC_{O111} on the left and EC_{O55} on the right). Both axes show normalized signal in a logarithmic (log2) scale. Blue lines delimit the twofold change. Insert shows close-up of the peptide microarray binding patterns of: A) EC_{O111} and B) EC_{O55}. The first six (of 20) amino acids are shown. (For a full sequence see the Supporting Information.)

(Table 2). The heat map shown in Figure 9 graphically demonstrates the expression levels of each of the EC1–8 and PA1–9 peptides in Qdot–PA_{10} and Qdot–EC_{O111} experiments. All EC peptides present a high expression in the EC_{O111} experiment, while the expression in the PA_{10} experiment is low. The opposite is true for PA peptides, which have high expression in the PA_{10} experiment, but low in the EC_{O111} experiment.

Structural considerations

As seen in Table 2, most of the peptides unique to EC_{O111} are enriched in aromatic tryptophan and cationic arginine, lysine, and histidine, while peptides specific to PA_{10} tend to contain aliphatic amino acids, anionic aspartic, and glutamic acids, and especially hydrogen bond forming glycine, proline, serine, and threonine (Figure S4). These differences are reflected in the consistent differences in pI values and aliphatic indices (AI) of the selected peptides (Table 2). This can be explained by the prominent compositional differences between EC_{O111} and PA_{10} LPS. Interestingly, Cherkasov et al.[39] recently found the same kind of amino acid distribution by using artificial intelligence in the design of peptide antibiotics.

As shown in Figure 7, the O-antigens of EC_{O111} and EC_{O55} LPS are dominated by neutral galactose-like structures, such as colitose, galactose, and galactosamine. The aromatic amino acids, W, F, or Y, are known to interact with the nonpolar b-face of galactose to provide a common binding motif residue for most galactose-binding proteins.[40,41] So, it is not unusual that the EC_{O111} binding peptides show a high incidence of aromatic amino acids, such as tryptophan, phenylalanine, and tyrosine. These observations are further supported by two independent investigations. In one study, peptides were selected to bind components of the bacterial cell membrane devoid of polysaccharides. This selection led to peptides containing only cationic arginine and lysine, but no aromatic residues.[42] In a second study, peptides that bind LPS from *S. enterica* (LPSs from *E. coli* and *S. enterica* are closely related)[37] were identified by screening phage displayed peptide libraries against bead-immobilized LPS.[43] All of these peptides were found to be enriched in aromatic hydrophobic residues, such as tryptophan and phe-

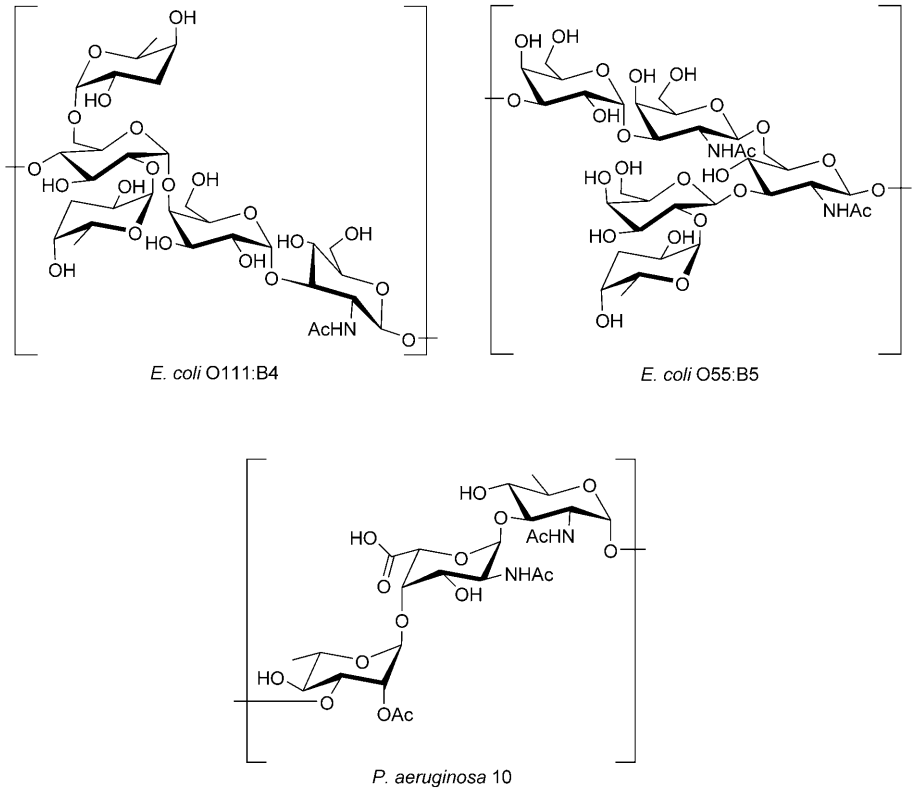

Figure 7. Chemical structures of the repeating units of LPS used in this work.[36–38]

nylalanine, along with cationic residues. These peptides were capable of discriminating between various bacterial species, which strongly supports their ability to target the distinctly variable O-antigenic domains.

In contrast to the neutral EC_{O111} and EC_{O55} repeating units, the repeating unit of PA_{10} consists one third of negatively charged galacturonic acid (Figure 7), which can form strong hydrogen bonds with the aspartic and glutamic acids,[44] as well as with hydrophilic glycine, proline, serine, and threonine, which are prominently over-represented in the selected PA_{10}-specific peptides (Figure S4).

Electrostatic contributions

To test the contribution of electrostatic interactions to LPS binding to microarray peptides, we measured the zeta potential (ζ-potential) of EC_{O111} and PA_{10} LPS. The zeta potential is the overall charge a particle acquires in a specific medium and is a measure of the potential at the slipping plane, which is the layer just past the bulk solution layer of ions surrounding the particle. Under conditions identical to those used in the microarray probing experiments, the EC_{O111} LPS had a charge of $\zeta = (-6.7 \pm 1.4)$ mV, while the PA_{10} LPS was also negative and of significantly greater magnitude at $\zeta = (-25.7 \pm 3.1)$ mV, which is consistent with the presence of negatively charged galacturonic acid. Since the EC_{O111} LPS has only hydroxyls in the structure and thus lacks the ability to form strong hydrogen bonds in aqueous solutions,[45] its interactions are dominated by CH–π interactions[45] and by electrostatic attraction, which drive the selection towards hydrophobic aromatic and cationic amino acids. On the other hand, the galacturonic acid in the repeating unit of PA_{10} LPS has a strong propensity to form hydrogen bonds, which overpowers the electrostatic forces and drives the selection towards hydrogen-bond-forming amino acids.

We conclude that specific interactions of peptides with LPS on microarrays are not driven by electrostatic forces alone, but involve far more specific molecular interactions, such as hydrogen bonds and hydrophobic forces. This makes the peptide microarray a suitable tool for studying carbohydrate interactions.

Conclusions

In summary, we have developed a LPS screening technology to quickly identify LPS binding peptides that are specific to the variable saccharidic branch of LPS. We demonstrated that such a platform, which consists of only 10000 random 20-mer sequences, is capable of differentiating between Gram-negative bacterial strains based on differences in their LPS structures. We also demonstrated that the parallel analysis platform, inherent to the microarray format, allows rapid and, most important, direct identification of multiple LPS interactions at the same time. In contrast to screening of phage displayed or other solution-based combinatorial peptide libraries, microarray format allows systematic analysis and statistical deconvolution of postselection data. In the future, as peptide microarray technology matures and the number of features increases, this platform could enable direct discovery of high-affinity and protease-resistant peptidomimetics since peptides can be readily synthesized with unnatural functionalities, for example, D-amino acids, cyclic structures, and unnatural side chains, to facilitate the transition of discovered leads into the clinic. Finally, this technology paves the way for systematic investigation of disease-associated changes in other poorly defined complex glycobiomolecules, such as mucins and glycosylaminoglycans that currently present insurmountable challenges to the available analytical methods.

Experimental Section

Materials and methods: Smooth-type LPS from *E. coli* serotype O111:B4 was obtained from Fluka (Cat# 62325), serotype O55:B5

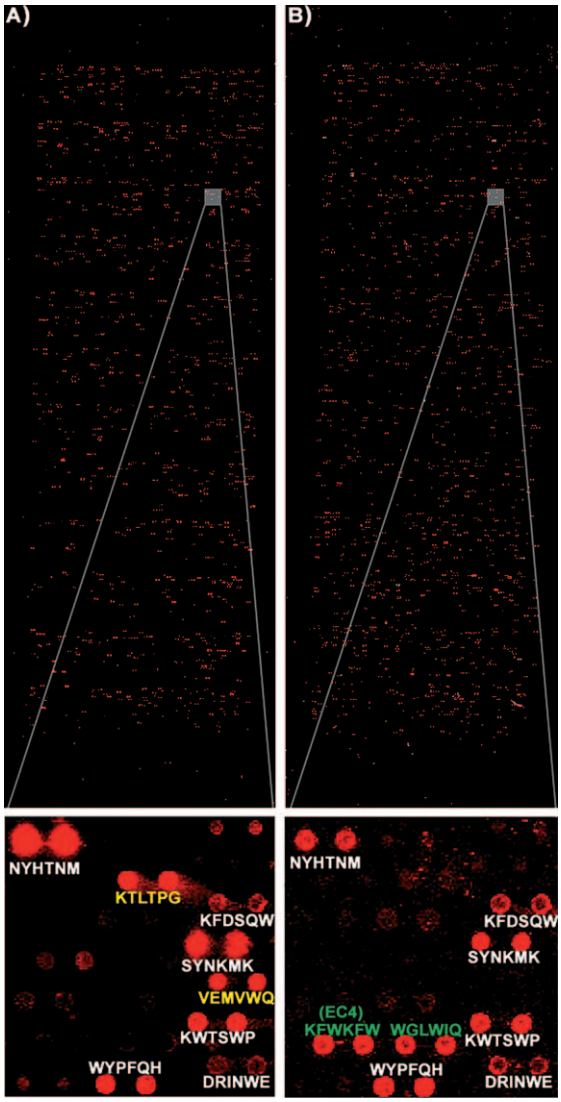

Figure 8. LPS binding patterns ("glycosignatures") on the microarray of: A) *P. aeruginosa* 10 LPS and B) *E. coli* O111:B4 LPS. Sequences in yellow indicate peptides unique to *P. aeruginosa*; sequences in green are unique to *E. coli*; sequences in white are common binders. Only the first six (of 20) amino acids are shown. (For a full sequence see the Supporting Information.)

was from Sigma (Cat# 62326); *P. aeruginosa* 10 was from Sigma (Cat# L8643). FITC-labeled LPS from *E. coli* O111:B4 was from Sigma (Cat# F3665). ***CAUTION!*** LPS molecules are highly pyrogenic and can cause severe fever in humans if inhaled, ingested, or absorbed through skin. Good laboratory practices should be employed. Wear a lab coat, gloves, safety glasses, and a respiratory mask while handling LPS.

Unless noted otherwise, all chemicals were purchased from Sigma–Aldrich, Inc. (Milwaukee, WI, USA) and used without further purification. Deionized water was obtained from a Millipore ultrapure water filtration unit. PEPscreen® peptides were synthesized by Sigma–Genosys, Inc., with 100% quality control and used as received for initial screens. Lead peptides were resynthesized in-house by using Fmoc chemistry and purified to 95% by HPLC. Organic Qdots® were purchased from Invitrogen (Carlsbad, CA, USA; Cat# Q21701MP). Sephacryl H*i*Prep 16/60 (S-200 HR) was from GE Healthcare. In-solution nanosizing and zeta potential was measured by using a Zetasizer Nano-ZS instrument (Malvern Instruments, Worcestershire, UK). Spectrophotometric measurements were carried out by using a NanoDrop® ND-1000 instrument.

Labeling LPS with Qdots: The supplied solution of organic Qdots (QDot 605 ITK™, Cat# Q21701MP, Invitrogen, Inc.) in decane (1 μM) was evaporated to dryness by using a SpeedVac® at room temperature and redissolved in equal amount of chloroform. An aliquot (100 μL) of the chloroform solution was diluted to 500 μL with chloroform and mixed with an aqueous solution of corresponding LPS (100 μL of 10 mg mL^{-1}; *E. coli* O111:B4, *E. coli* O55:B5, and *P. aeruginosa* 10). Methanol was added dropwise and the sample was occasionally vortexed until both phases were completely mixed (about 400 μL of MeOH). The mixture was then evaporated to dryness by using a SpeedVac and the solid residue was suspended in ddH_2O (100 μL). A saturated solution of tetramethylammonium hydroxide pentahydrate ($Me_4NOH \times 5H_2O$) was added until the mixture was at pH 11–12 (about 25 μL). The latter basification step is critical as it allows the transfer of the Qdots into the aqueous phase; no transfer occurs in nonbasified solutions. The mixture was sonicated for 30 min, and the colored solution was then passed through two consecutive Zeba columns (2 mL; Pierce) to remove salts and excess free LPS. We further purified the LPS-coated Qdots by size-exclusion chromatography using Sephacryl H*i*Prep 16/60 (S-200 HR) column (50×1 cm). The Qdot–LPS constructs eluted in a narrow color band and were stored in the dark at 4 °C. Under these conditions, the Qdot–LPS are stable for at least one month without any visible signs of deterioration. In a control experiment, the above procedure was repeated without LPS. No solubilization of Qdots was observed without LPS as determined by measuring absorbance of Qdots in the supernatant.

Peptide microarray design and construction: The peptide microarray consisted of 10000, 20-residue peptides of random sequence, with a C-terminal linker of –Gly-Ser-Cys-COOH. All peptides were synthesized by Alta Biosciences Ltd. (Birmingham, UK) based on amino acid sequences provided by in-house custom software (Hunter, Preston, and Uemura, Yusuke, CIM, The Biodesign Institute). Nineteen amino acids (cysteine was excluded) were selected at random for each of the first seventeen positions with –GSC as the carboxy-terminal linker. The synthesis scale was 2–5 mg total at ≥70% purity and 2% of the peptides were tested at random by mass spectrometry as quality control. Dry peptides were dissolved in *N*,*N*′-dimethylformamide (100%), then diluted 1:1 with purified water at pH 5.5 to a master concentration (2 mg mL^{-1}). The original 96-deep-well plates were robotically transferred to 384-well spotting plates, and the peptides were diluted to a final spotting concentration (1 mg mL^{-1}) in phosphate buffered saline at pH 7.2. High-quality precleaned Gold Seal glass microscope slides were obtained from Fisher (Fair Lawn, NJ, USA; Cat# 3010). Each slide was treated with amino-silane, activated with sulfo-SMCC (Pierce Biotechnology, Rockford, IL, USA; Cat# 22622) to create a maleimide-activated surface, and the quality was checked for coating efficiency. During spotting, we employed a Telechem Nanoprint 60 using 48 Telechem series SMP2 style titanium pins. Each pin spots approximately 500 pL of peptide (1 mg mL^{-1}) per spot—an estimate based on pin trajectory, surface dwell time, and the amount of liquid each pin holds. The spotting environment was at 25 °C and 55% humidity. The maleimide-activated surface reacts with the sulfhydryl group on the peptide's terminal cysteine. Each peptide was spotted twice per array. The arrays were spotted in an orange-crate packing pattern to maximize spot density. Six fiducials were applied asymmetrically by using AlexaFluor647, -555, and -488 la-

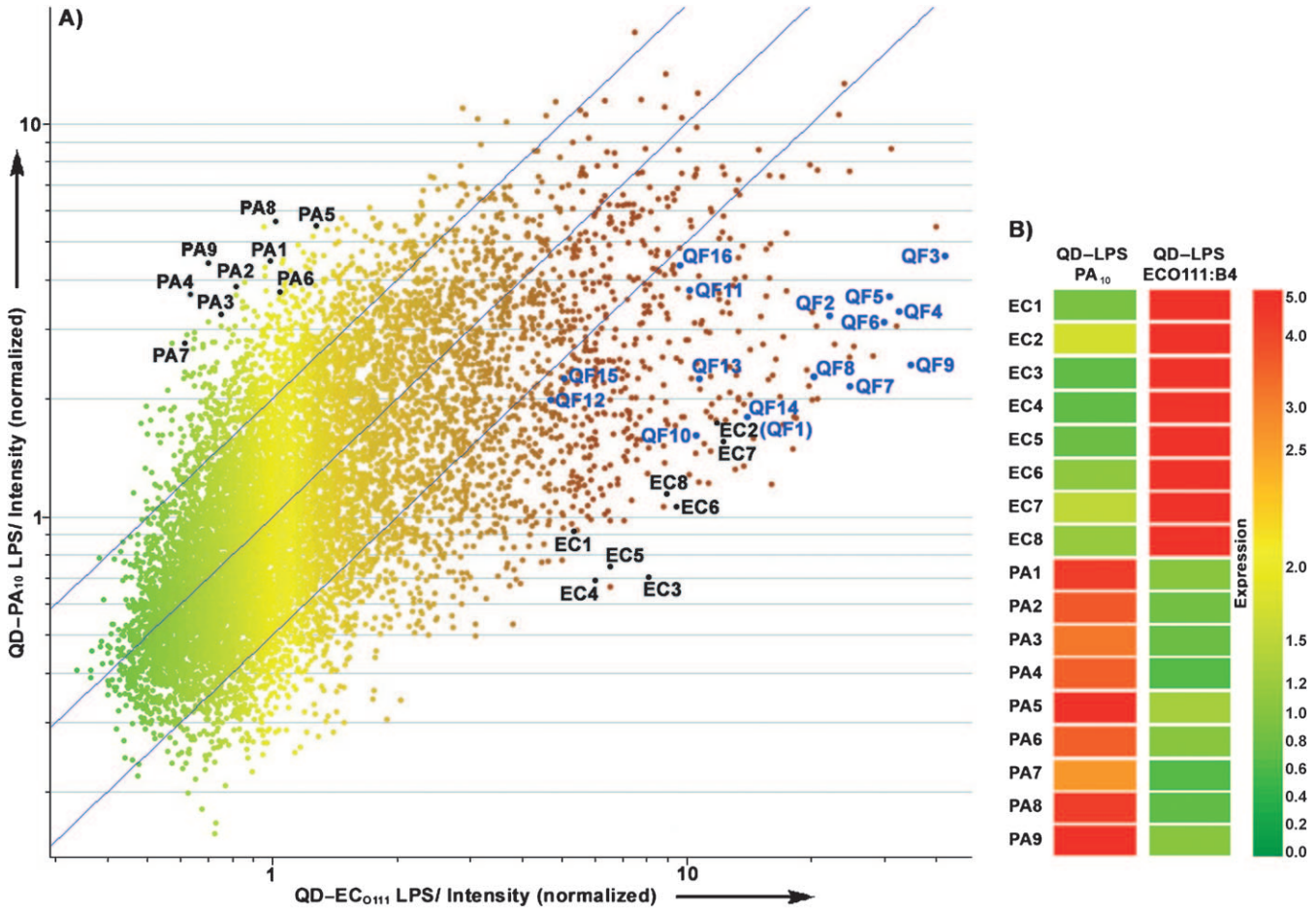

Figure 9. A) *E. coli* O111:B4 versus *P. aeruginosa* 10 LPS correlation ($R = 0.630$). Annotated blue dots correspond to peptides shown in Table 1; annotated black dots correspond to the peptides shown in Table 2. Both axes show normalized fluorescence signal at 605 nm on a logarithmic scale. Blue lines delimit the twofold change. B) Heat map compares the level of expression (luminescent intensity, log2) for the EC and PA peptides (green: low; red: high).

Table 2. Peptides specific to EC LPS versus PA_{10} LPS. Column headings indicate the isoelectric point (pI), negative residues (NR), positive residues (PR), and aliphatic index (AI).

ID	Peptide sequence	Qdot–EC_{O111}	Qdot–EC_{O55}	Qdot–PA_{10}	pI	NR	PR	AI
EC1	KFWHHKWWHWFKWRRRRGSC	+	+	–	12.0	0	7	0
EC2	RHWRKPRKWHKKWPPHRGSC	+	+	–	12.0	0	8	0
EC3	HHFKHHRHWKRRRHWFWGSC	+	+	–	12.0	0	6	0
EC4	KFWKFWHKHRHRHRWHRGSC	+	+	–	12.0	0	7	0
EC5	HRWWFKKKHRFRWWKRWGSC	+	+	–	12.0	0	8	0
EC6	WRHWRRRKHFWWKRRWHGSC	+	+	–	12.3	0	8	0
EC7	GWAREHHWPRIIYGVLRGSC	+	+	–	9.5	1	3	78
EC8	HHPRHWWWKRWHPFRFFGSC	+	+	–	11.7	0	4	0
PA1	VPTPNDQGKQWVNSVNAGSC	–	–	+	5.8	1	1	49
PA2	RKHDYEEVESEFHPRKGGSC	–	–	+	6.0	5	4	15
PA3	SHPRITTSDDHGDSPKGGSC	–	–	+	5.9	3	2	20
PA4	VPVHDKTRKTAPAEEIVGSC	–	–	+	6.7	3	3	73
PA5	GSSMHHHPLWPTPEPHTGSC	–	–	+	6.4	1	0	20
PA6	RGMFHSPGDVMETEPHVGSC	–	–	+	5.3	3	1	29
PA7	WIEVEKTMDSGSGPKGHGSC	–	–	+	5.5	3	2	34
PA8	MTGIWSAMPYHNIESHNGSC	–	–	+	5.9	1	0	44
PA9	SHGNNQSHPEAYPGPWTGSC	–	–	+	5.9	1	0	5

beled peptides. The fiducials were used to align each subarray during image processing. The printed slides were stored under an argon atmosphere at 4 °C until used. Quality control included imaging the arrays by laser scanner (Perkin–Elmer ProScanArray HT, Perkin–Elmer, Wellesley, MA, USA) at 647 nm to image the spot morphology. If the batch passed this test, further testing of randomly selected slides with known proteins and antibodies was carried out for the quality control of precision spot intensity. Array

batches that failed to meet an array-to-array variability of 30% CV (coefficient of variation) were discarded.

Microarray probing: Each microarray probing was performed in triplicate. The slides were placed in a humidified chamber and blocked for 1 h at room temperature with BSA (650 μL of 3% solution) and methoxytetraethyleneglycol thiol ($mPEG_4$-SH; 1 mM)[46] in 1×PBS with Tween-20 (TBS-T; 0.05%). The slides were washed with 1xTBS-T (3×30 inversion in a Coupling jar) and ddH_2O (3×30 inversion in a Coupling jar). The slides were then dried by centrifugation at 1500 rpm for 3 min, with the barcode label at the bottom to avoid the spread of the label glue onto the slide surface. The slides were then scanned at the appropriate wavelength to note any peptide autofluorescence. An AbGene frame was then attached to the surface of each slide to confine the solution (260 μL) of labeled LPS in 1xPBS (0.154 mg mL^{-1} for FITC–LPS or AF488–LPS and 0.630 mg mL^{-1} for Qdot–LPS) that was added to the printed area. A plastic coverslip was used to spread the solution on the surface of the slide and seal the frame while avoiding bubbles. The slides were incubated for 1 h in the dark at room temperature in a humidified chamber. The coverslips and AbGene frames were then removed, and the slides were washed by being dipped two times in ddH_2O, then incubated for 5 min in ddH_2O, and then dipped two more times in ddH_2O; the solution was changed each time. Finally the slides were dried by centrifugation at 1500 rpm for 3 min at room temperature and scanned.

Microarray scanning and image analysis: Microarrays were scanned by using a Perkin–Elmer ProScanArray HT Microarray Scanner with the 488 and 543 nm excitation lasers at 100% power and 70% photomultiplier tube gain. Detection was done at 605 nm for Qdot probes and at 543 nm for FITC probes. All scanned images were analyzed by using GenePix Pro 6.0 software (Axon Instruments, Union City, CA, USA). Upon careful visual inspection, bad spots were eliminated by flagging them "absent". Median spot intensities were used in further analyses. Statistical analysis comparison of microarray data was done with GeneSpring 7.2 (Agilent, Inc., Palo Alto, CA, USA) by importing image-processed data from GenePix Pro 6.0 (Molecular Devices, Inc.). Median signal intensities were used in the calculations. For statistical comparisons, each slide was normalized to 50th percentile. Measurements of less than 0.01 were set to 0.01; per "gene" normalization were not included since it tends to overemphasize differences in peptide expression, even when the intensity value is almost negligible for all the experiments. However, the goal of this work is to differentiate peptides that show a distinct behavior towards different probes, not only by statistical means, but also by visual inspection of the slides. Autofluorescent peptides were identified by scanning the slides prior to binding with LPS, peptides which had fluorescent intensities comparable to the postbinding intensity were eliminated from the final selections. The results collected for each experiment were represented by using scatter plots as previously reported by Reddy and Kodadek.[24] This representation helped us focus our attention only on peptides with the right expression profile, that is, either with high expression against one of the LPSs tested and low expression for the other LPS, or with high expression for both.

Antimicrobial assays: DH10B *E. coli* cells (MAX Efficiency® DH10B™ Competent Cells, Cat# 18297-010, Invitrogen Inc.) were grown, overnight, at 37 °C at 270 rpm rotation in LB medium with streptomycin (0.1%) to a cell density of 2000×10^6 CFU mL^{-1}. An aliquot (1 μL) of these cultured cells was then mixed with fresh medium (1 mL) containing an individual peptide at concentrations of 25, 50 and 100 μM, and allowed to grow, overnight. The McFarland turbidity scale for *E. coli*[47,48] was used to quantify the overnight growth of the cells by comparing the optical density of the cells at 600 nm to the turbidity equivalent of $BaCl_2$ (1%)/H_2SO_4 (1%) in the microplate reader (Spectra MAX 190, Molecular Devices, Inc.). In control experiments, the above procedure was repeated with no peptide in the culture and with nonbinding peptide (Neg1, sequence EFSNPTAQVFPDFWMSDGSC) as a negative control.

Flow cytometry: Peptides were conjugated to biotin by incubation with heterobifunctional maleimide-PEO_2-biotin linker (Pierce Biotechnology, Inc.; Cat# 21901) in 1×PBS at pH 7.2, overnight, at room temperature. Excess biotin was removed by overnight dialysis by using 1 kDa cutoff membrane (Spectrum Laboratories, Inc.). *E. coli* DH10B (MAX Efficiency® DH10B™ Competent Cells, Cat# 18297-010, Invitrogen Inc.) were cultured under routine conditions, pelleted by centrifugation and washed (3×1×PBS) to remove traces of media. The harvested cells were resuspended in blocking buffer (1×PBS, 0.05% FBS). Experiments with LPS preincubation involved mixing biotinylated peptide solution (400 μM; 10 μL) with LPS solution (200 μM; 20 μL) for 1 h at room temperature. Then, 10×10^6 cells were mixed with biotinylated peptides (400 μM; 10 μL), biotinylated peptides preincubated with LPS, or biotinylated wheat germ agglutinin (WGA) lectin (EY Laboratories, Inc.; 10 μL of 1 mg mL^{-1} solution) and incubated for 1 h on ice. The cells were then washed three times with blocking buffer (1 mL) to remove unbound peptides or lectins. For detection of bound peptides and lectins, streptavidin–AlexaFluor488 (4 μg mL^{-1}, 100 μL; Invitrogen, Inc., Cat# S-11223) was added to the cells and incubated for 1 h. Cells were washed three times in blocking buffer, resuspended in blocking buffer (300 μL) and analyzed for cell-surface staining by using the FACS Caliber machine (BD Biosciences, Inc.). Cells stained with streptavidin–AlexaFluor488 only, were used as controls.

Surface plasmon resonance: Bare gold SPR sensor chips (Biosensing Instruments, Tempe, AZ, USA) were functionalized by adding 8-amino-1-octanethiol (1 mM; Dojindo Molecular Technologies, Inc., Cat# A424) in ddH_2O to the ethanol prewashed gold surface and incubating for 2 h at room temperature in a humidified chamber. The surface was then washed with ddH_2O and dried by using ultrapure argon gas. A solution of sulfo-SMCC linker (1 mM; bioWORLD, Dublin, OH, USA) in 1×PBS was added to the gold surface, incubated for 30 min at room temperature in a humidified chamber, then washed and dried as above. The SPR instrument sensitivity was calibrated by using the response from ethanol (1%) in water on a bare gold sensor chip as a standard. The AOT/sulfo-SMCC modified chip was mounted on the instrument, and the peptide was immobilized in the sample channel by injecting a solution of peptide (100 μM) in TBS-T. A solution of sodium dodecylsulfate (0.01%; SDS) in TBS-T was injected to dissociate any peptide aggregates. The SPR response after the SDS wash was used to calculate the immobilization density, where 1 RU = 1 pg mm^{-2}. To abrogate possible unspecific interactions, a solution of $mPEG_4$-SH (1 mM)[46] was used to block unreacted maleimide groups on the sample channel and to act as a nonbinding control on the reference channel. A solution of LPS (1 mg mL^{-1}) from *E. coli* serotype O111:B4 was injected at 20 μL min^{-1} flow rate in the TBS-T analyte solution. Regeneration was accomplished by using SDS (0.05%) followed by an injection of glycine (10 mM; pH 2.5).

LPS zeta potential (ζ-potential) and size measurements: The zeta potential of the LPS was determined by electrophoretic mobility by using a Zetasizer Nano-ZS (Malvern Instruments). Measurements were performed at 25 °C in clear disposable Zeta cells (Malvern Instruments). LPS concentrations were the same as the ones used in the microarray probing experiments. All measurements were done in triplicate.

ITC measurements:[34] LPS was dissolved in PBS, pH 7.4, to give a 75 μM solution (assumed $M_W = 10\,000$ kDa) equilibrated by dialysis, overnight, and degassed under vacuum. The QF8 peptide was dissolved in the same buffer at 1 mM and degassed under vacuum. Isothermal calorimetric titrations were performed by using the Nano ITC (TA Instruments, New Castle, DE, USA) at 23.5 °C. Degassed LPS (0.075 mM) was loaded into the sample cell (volume 950 μL), the reference cell was filled with water, and the degassed QF8 peptide (1 mM) was loaded into the injection syringe. Aliquots of QF8 (20×5 μL) were titrated into the LPS in the reaction cells at an interval of 300 s while being stirred at 150 rpm. Raw data were corrected for the heat of dilution of QF8 into buffer and integrated by using NanoAnalyze 1.1.0 software. The independent binding model allowed the determination of the binding stoichiometry (n), association constant (K_a), and enthalpy change (ΔH). The free energy (ΔG) and enthalpy (ΔS) changes were calculated through the fundamental equations of thermodynamics: $\Delta G = -RT\ln K_a$ and $\Delta S = (\Delta H - \Delta G)T^{-1}$, respectively. All titration curves were repeated at least three times.

Acknowledgements

The work was funded by the Arizona Technology and Research Initiative Funds to S.A.S. and S.A.J. and by the Wallace Foundation grant AI057156 to S.A.J. Dr. Jose Cano Buendia and Dr. Miti Shah are thanked for help with antimicrobial assays. Dr. David W. Thomas (TA Instruments) is acknowledged for help with ITC interpretation.

Keywords: bacterial lectins · microarrays · mimetics · peptides · polysaccharides

[1] J. E. Turnbull, R. A. Field, *Nat. Chem. Biol.* **2007**, *3*, 74–77.
[2] C. Ortiz Mellet, J. M. Garcia Fernandez, *ChemBioChem* **2002**, *3*, 819–822.
[3] K. T. Pilobello, L. K. Mahal, *Curr. Opin. Chem. Biol.* **2007**, *11*, 300–305.
[4] K. T. Pilobello, L. Krishnamoorthy, D. Slawek, L. K. Mahal, *ChemBioChem* **2005**, *6*, 985–989.
[5] K. L. Hsu, L. K. Mahal, *Nat. Proteins* **2006**, *1*, 543–549.
[6] K. T. Pilobello, D. E. Slawek, L. K. Mahal, *Proc. Natl. Acad. Sci. USA* **2007**, *104*, 11534–11539.
[7] J. C. Manimala, Z. T. Li, A. Jain, S. VedBrat, J. C. Gildersleeve, *ChemBioChem* **2005**, *6*, 2229–2241.
[8] T. Kodadek, *Chem. Biol.* **2001**, *8*, 105–115.
[9] M. Cacciarini, E. Cordiano, C. Nativi, S. Roelens, *J. Org. Chem.* **2007**, *72*, 3933–3936.
[10] Y. Ferrand, M. P. Crump, A. P. Davis, *Science* **2007**, *318*, 619–622.
[11] M. Mazik, H. Cavga, P. G. Jones, *J. Am. Chem. Soc.* **2005**, *127*, 9045–9052.
[12] M. Dowlut, D. G. Hall, *J. Am. Chem. Soc.* **2006**, *128*, 4226–4227.
[13] N. Y. Edwards, T. W. Sager, J. T. McDevitt, E. V. Anslyn, *J. Am. Chem. Soc.* **2007**, *129*, 13575–13583.
[14] S. A. Svarovsky, L. Joshi, *Curr. Drug Discovery Technol.* **2008**, *5*, 20–28.
[15] S. A. David, *J. Mol. Recognit.* **2001**, *14*, 370–387.
[16] S. J. Wood, K. A. Miller, S. A. David, *Comb. Chem. High Throughput Screening* **2004**, *7*, 733-743.
[17] J. Balzarini, *Nat. Rev. Microbiol.* **2007**, *5*, 583–597.
[18] M. Caroff, D. Karibian, *Carb. Res.* **2003**, *338*, 2431–2447.
[19] K. Triantafilou, M. Triantafilou, N. Fernandez, *Cytometry* **2000**, *41*, 316–320.
[20] U. Resch-Genger, M. Grabolle, S. Cavaliere-Jaricot, R. Nitschke, T. Nann, *Nat. Methods* **2008**, *5*, 763–775.
[21] B. Dubertret, P. Skourides, D. J. Norris, V. Noireaux, A. H. Brivanlou, A. Libchaber, *Science* **2002**, *298*, 1759–1762.
[22] R. E. Anderson, W. C. W. Chan, *ACS Nano* **2008**, *2*, 1341–1352.
[23] J. L. Ding, P. Li, B. Ho, *Cell. Mol. Life Sci.* **2008**, *65*, 1202–1219.
[24] M. M. Reddy, T. Kodadek, *Proc. Natl. Acad. Sci. USA* **2005**, *102*, 12672–12677.
[25] C. J. C. de Haas, H. J. van Leeuwen, J. Verhoef, K. P. M. van Kessel, J. A. G. van Strijp, *J. Immunol. Methods* **2000**, *242*, 79–89.
[26] J. J. Lundquist, E. J. Toone, *Chem. Rev.* **2002**, *102*, 555–578.
[27] M. Mancek, P. Pristovsek, R. Jerala, *Biochem. Biophys. Res. Commun.* **2002**, *292*, 880–885.
[28] D. I. Chan, E. J. Prenner, H. J. Vogel, *Biochim. Biophys. Acta Biomembr.* **2006**, *1758*, 1184–1202.
[29] Z. Wang, G. S. Wang, *Nucl. Acids Res.* **2004**, *32*, D590–D592.
[30] S. Lata, B. K. Sharma, G. P. S. Raghava, *BMC Bioinformatics* **2007**, *8*, 263.
[31] Y. Rosenfeld, H. G. Sahl, Y. Shai, *Biochemistry* **2008**, *47*, 6468–6478.
[32] Q. P. Lin, L. F. Zhou, N. N. Li, Y. Q. Chen, B. C. Li, Y. F. Cai, S. Q. Zhang, *Eur. J. Pharmacol.* **2008**, *596*, 160–165.
[33] K. J. Foley, E. S. Forzani, L. Joshi, N. Tao, *Analyst* **2008**, *133*, 744–746.
[34] A. Bhunia, G. L. Chua, P. N. Domadia, H. Warshakoon, J. R. Cromer, S. A. David, S. Bhattacharjya, *Biochem. Biophys. Res. Commun.* **2008**, *369*, 853–857.
[35] K. Brandenburg, I. Moriyon, M. D. Arraiza, G. Lewark-Yvetot, M. H. J. Koch, U. Seydel, *Thermochim. Acta* **2002**, *382*, 189–198.
[36] R. K. Gupta, W. Egan, D. A. Bryla, J. B. Robbins, S. C. Szu, *Infect. Immun.* **1995**, *63*, 2805–2810.
[37] G. Samuel, J. P. Hogbin, L. Wang, P. R. Reeves, *J. Bacteriol.* **2004**, *186*, 6536–6543.
[38] Y. A. Knirel, O. V. Bystrova, N. A. Kocharova, U. Zahringer, G. B. Pier, *J. Endotoxin Res.* **2006**, *12*, 324–336.
[39] A. Cherkasov, K. Hilpert, H. Jenssen, C. D. Fjell, M. Waldbrook, S. C. Mullaly, R. Volkmer, R. E. W. Hancock, *ACS Chem. Biol.* **2009**, *4*, 65–74.
[40] K. Drickamer, *Structure* **1997**, *5*, 465–468.
[41] M. S. Sujatha, P. V. Balaji, *Proteins Struct. Funct. Bioinf.* **2004**, *55*, 44–65.
[42] Q. H. Xie, S. Matsunaga, Z. S. Wen, S. Niimi, M. Kumano, Y. Sakakibara, S. Machida, *J. Pept. Sci.* **2006**, *12*, 643–652.
[43] Y. G. Kim, C. S. Lee, W. J. Chung, E. M. Kim, D. S. Shin, J. H. Kim, Y. S. Lee, J. H. Chung, B. G. Kim, *Biotechnol. Lett.* **2006**, *28*, 79–84.
[44] J. H. Chen, C. L. Brooks, H. A. Scheraga, *J. Phys. Chem. B* **2008**, *112*, 242–249.
[45] A. P. Davis, R. S. Wareham, *Angew. Chem.* **1999**, *111*, 3160–3179; *Angew. Chem. Int. Ed.* **1999**, *38*, 2978–2996.
[46] M. Zheng, Z. G. Li, X. Y. Huang, *Langmuir* **2004**, *20*, 4226–4235.
[47] A. L. Koch in *Methods for General and Molecular Bacteriology* (Ed.: P. Gerhardt), American Society for Microbiology, Washington DC, **1994**, pp. 248–277.
[48] R. M. Smibert, N. R. Keig in *Methods for General and Molecular Bacteriology* (Ed.: P. Gerhardt), American Society for Microbiology, Washington DC, **1994**, pp. 607–654.

Received: November 1, 2008
Published online on February 26, 2009

